Dissecting the Molecular Response of Human Escs to Iron-Mediated Oxidative Stress by Genetic Silencing of *FTH1* Gene

Luana Scaramuzzino
Magna Græcia University of Catanzaro Department of Experimental and Clinical Medicine: Universita degli Studi Magna Graecia di Catanzaro Dipartimento di Medicina Sperimentale e Clinica

Valeria Lucchino
Magna Græcia University of Catanzaro Department of Experimental and Clinical Medicine: Universita degli Studi Magna Graecia di Catanzaro Dipartimento di Medicina Sperimentale e Clinica

Stefania Scalise
Magna Græcia University of Catanzaro Department of Experimental and Clinical Medicine: Universita degli Studi Magna Graecia di Catanzaro Dipartimento di Medicina Sperimentale e Clinica

Michela Lo Conte
Magna Græcia University of Catanzaro Department of Experimental and Clinical Medicine: Universita degli Studi Magna Graecia di Catanzaro Dipartimento di Medicina Sperimentale e Clinica

Clara Zannino
Magna Græcia University of Catanzaro Department of Experimental and Clinical Medicine: Universita degli Studi Magna Graecia di Catanzaro Dipartimento di Medicina Sperimentale e Clinica

Alessandro Sacco
Magna Græcia University of Catanzaro Department of Experimental and Clinical Medicine: Universita degli Studi Magna Graecia di Catanzaro Dipartimento di Medicina Sperimentale e Clinica

Flavia Biamonte
Magna Græcia University of Catanzaro Department of Experimental and Clinical Medicine: Universita degli Studi Magna Graecia di Catanzaro Dipartimento di Medicina Sperimentale e Clinica

Elvira Immacolata Parrotta (✉ parrotta@unicz.it)
University of Catanzaro Magna Graecia Department of Medical and Surgical Sciences: Universita degli Studi Magna Graecia di Catanzaro Dipartimento di Scienze Mediche e Chirurgiche
https://orcid.org/0000-0001-8145-3623

Francesco Saverio Costanzo
Magna Græcia University of Catanzaro Department of Experimental and Clinical Medicine: Universita degli Studi Magna Graecia di Catanzaro Dipartimento di Medicina Sperimentale e Clinica

Giovanni Cuda
Magna Græcia University of Catanzaro Department of Experimental and Clinical Medicine: Universita degli Studi Magna Graecia di Catanzaro Dipartimento di Medicina Sperimentale e Clinica

Research Article

Keywords: Human embryonic stem cells (hESCs), FTH1, redox regulation, oxidative stress, Nrf2, metabolic rerouting.

Posted Date: July 28th, 2021

DOI: https://doi.org/10.21203/rs.3.rs-741242/v1

Abstract

Background: Embryonic stem cells (ESCs) are pluripotent cells with indefinite self-renewal ability and differentiation properties. As such, to function properly and maintain genomic stability, ESCs need to be endowed with an efficient repair system as well as effective redox homeostasis. In this study, we investigated and characterized different aspects involved in ESCs response to iron accumulation following stable knockdown of ferritin heavy chain (*FTH1*) gene, encoding for a major iron storage protein with ferroxidase activity.

Methods: stable *FTH1* knockdown of H9-hES cell line was achieved with the use of shRNA lentiviral particles. Upon FTH1 silencing, we speculated whether hESCs still retained their pluripotency capability were first monitored for their capability the pluripotent status,FTH1 stable knock-down ESCs were obtained using lentiviral vector plasmids. The effect of FTH1 silencing on hESCs pluripotency was evaluated through alkaline phosphatase (AP) staining, immunofluorescence and embryoid bodies (EBs) formation assay. Western blotting and qRT-PCR analysis were performed to assess the involvement of nuclear factor (erythroid-derived-2)-like 2 (Nrf2) and pentose phosphate pathway (PPP) in the antioxidant response. ROS levels and mitochondrial functionality were explored by flow cytometry. Seahorse Analyzer was used to evaluate metabolic and bioenergetic profiles.

Results*:* Our findings clearly show that *FTH1* silencing in hESCs does not correlate with increased ROS production nor with redox status strengthening the concept that hESCs are extremely resistant and, to certain extent, even refractory to the pattern of results produced in other cell lines. Collectively, our results demonstrate that *FTH1* silencing is accompanied by a significant activation of the nuclear factor (erythroid-derived-2)-like 2 (Nrf2) signaling pathway and pentose phosphate pathway (PPP) which crosstalk in driving hESCs antioxidant cascade events able to antagonize the effects of FTH1 silencing.

Conclusion: to our knowledge, this is the first evidence of a crosstalk between *FTH1* silencing and Nrf2 pathway activation in hESCs, casting a new light on how human ESCs perform under oxidative stress conditions. Our findings go beyond previous reports, showing how the Nrf2 pathway, in combination with PPP activation, regulates the molecular signature underlying ESCs defence mechanisms against oxidative stress mediated by *FTH1* downregulation.

Introduction

An impaired cellular balance between reactive oxygen species (ROS) production and clearance is responsible for establishing an oxidative stress status leading to lethal consequences (18) due to the toxic effects responsible for damage in many cellular components, including DNA. Depending on time and concentration, ROS elicit a wide spectrum of responses; indeed, slight variation in ROS concentrations may have profound and opposite effects, such as cell survival and apoptosis (49). High levels of ROS, predominantly produced by the mitochondrial respiration, are classically linked to cellular damage, oxidative stress, DNA damage, and apoptosis, highlighting the importance of proper

functionality of iron-containing molecules (1). On the other hand, a large body of research recognizes ROS signaling to serve as second messenger critically involved in many biological processes, including DNA synthesis, gene expression, cellular respiration, protein-protein interactions (30), as well as activation of critical pathways such as protein kinase B (AKT) and NF-κB (88). In hESCs, constant exposure to high levels of ROS was shown to induce cell cycle arrest and apoptosis (22); however, by regulating the redox state, ROS also target important aspects of pluripotent ESCs, such as metabolism, self-renewal, and cell fate (19, 34, 66). During evolution, cells have developed specific and efficient antioxidant defence systems to promptly detoxify reactive intermediates and maintain redox homeostasis, fundamental against oxidative stress damage (76). The response to oxidative stress is cell-specific: some cell types are extremely sensitive while others, such ESCs, are instead endowed with robust and highly efficient repair systems (3, 22). ESCs are pluripotent stem cells characterized by unlimited self-renewal capacity and ability to give rise to cells of all three germ layers (ectoderm, mesoderm, and endoderm) naturally occurring during embryo development *in vivo*, or by differentiating culture conditions *in vitro* (52). As such, it is extremely important for ESCs to function properly and maintain genome stability. To do so, ESCs are equipped with enhanced repair systems and efficient redox homeostasis to preserve their functional properties and prevent dramatic consequences of oxidative stress (53). On the other hand, low levels of ROS production are required for ESCs to sustain their self-renewal ability (3, 69), while the increase in ROS was shown to favor ESCs differentiation (44, 68). Moreover, the canonical pluripotency core itself, including *OCT4*, *SOX2*, and *NANOG*, is responsible for regulating the expression of some important antioxidant genes, such as *SOD1*, suggesting a correlation between mechanisms governing pluripotency and antioxidant systems (71). To maintain high antioxidant activity, ESCs rely on low mitochondrial biogenesis and reduced oxygen consumption (17, 62, 85). The antioxidant system includes a wide range of enzymes such as those encoded by the superoxide dismutase family genes (*SODs*), glutathione peroxidase family (*GPXs*), and catalase (*CAT*). In addition, many other non-enzymatic molecules and compounds such as ascorbic acid, directly or indirectly, participate in antioxidant events (11). The redox status is greatly influenced by compounds primarily involved in the metabolism of specific substances, such as iron (20). Iron deficiency triggered by Deferoxamine (DFO) treatment was shown to be involved in loss of pluripotency both in ESCs and induced pluripotent stem cells (iPSCs) (25). On the other hand, increased intracellular iron levels also negatively affect the status of pluripotent stem cells (PSCs), leading to excess ROS production, DNA damage, and reduced proliferation rate (24). The role of ROS in sophisticated and finely regulated mechanisms such as pluripotency and differentiation has been described in many studies, but the real effects of ROS accumulation in ESCs and the underlying molecular mechanisms still remain imprecise; moreover, even less speculated is the role of unbalanced iron metabolism in hESCs, suggesting that much still remains to be investigated in this direction. PSCs mainly rely on glycolysis (42) while oxidative metabolism (mitochondrial respiration and fatty acid metabolism) take place upon PSCs differentiation (17, 46, 86). Reprogramming of somatic cells to generate iPSCs requires, among others, a metabolic switch from oxidative phosphorylation (OXPHOS) to glycolysis, strengthening the high dependency of PSCs on glycolytic metabolism (62). The prevailing aerobic over oxidative mitochondrial metabolism in PSCs is reminiscent of cancer metabolism (7, 28, 45, 62). As cancer cells, in fact, PSCs divide rapidly and, in order to sustain the high proliferation

rate, these cells are required to produce ATP from glycolysis even in the presence of normal oxygen levels. Glycolytic metabolism also generates nicotinamide adenine dinucleotide phosphate, NADPH that, in addition to being involved in sustaining the high proliferation rate, protects against oxidative stress (48). Additionally, as cancer cells, PSCs are characterized by an increased expression of hypoxia-inducible factors (HIFs) and oxygen-sensitive transcription factors. Nevertheless, oxidative mitochondrial metabolism was shown to be active in hESCs in particular conditions, such as high lipids, and metabolic flux analysis (MFA) demonstrating that PSCs can adapt their metabolism to various nutrient conditions while maintaining full self-renewal properties (84).

To push the PSCs technology towards clinical applications, a comprehensive understanding of stemness and its potentiality, as well as stem cells metabolism and its modulation are fundamental steps to be considered to generate PSC derivatives that faithfully recapitulate all aspects of somatic cells and tissues. While ESCs general metabolic aspects have been widely investigated (43, 77, 84), very little is currently known about the role of iron metabolism and the consequences of iron accumulation in hESCs. Based on these considerations, the present work speculates the molecular events triggered by silencing of the *FTH1* gene, encoding a major antioxidant protein with ferroxidase activity. We therefore analyzed key processes known to be associated with intracellular iron accumulation such as DNA damage, apoptosis, oxidative stress, antioxidant defence system, and metabolic changes. Our findings provide clear evidence of overactivation of the nuclear factor (erythroid-derived-2)-like 2 (Nrf2) signaling pathway as the major player and safeguard of hESCs against iron-mediated oxidative stress in response to downregulation of ferritin expression. From a metabolic point of view, we identified the pentose phosphate pathway (PPP) activation as the primary metabolic response to maintain the redox status in hESCs.

Material And Methods

Cell culture

H9 Embryonic Stem Cell line was obtained from WiCell Research Institute (Madison, WI, http://www.wicell.org). ESCs were propagated on Matrigel-coated (Corning, NY, 354277) dishes in StemMACS iPS-Brew medium (Miltenyi Biotec, Bergisch Gladbach, Germany, 130-104-368) and cultured at 37°C in 5% CO2 in a humidified incubator with daily medium replacement. Cells were subcultured as small colonies with Gentle Dissociation reagent (STEMCELL Technologies, Vancouver, BC, 07174).

Lentiviral production and generation of stable knock-down ESCs

Lentiviral particles were produced in 293T cells following standard procedure. Briefly, subconfluent 293T cells were transfected with shFTH1 or shSCR control lentiviral vector plasmids (Sigma-Aldrich, St. Louis, MO) along with pCMV-DR9-9 and pCMV-VSVG plasmids (Sigma-Aldrich). After 48 hours, supernatants were harvested, filtered through a 0.45 µM filter, and used for ESCs infection, previously seeded in a 6-well plate at a cell density of $2x10^5$ cells/well. Infected cells were incubated with sh*FTH1* and shSCR control

lentiviral particles [Multiplicity of Infection (MOI) = 10] in the presence of 8 µg/ml of Polybrene (Sigma-Aldrich) using Lipofectamine 3000 Reagent (Thermo Fisher Scientific, Waltham, MA). Two days after transduction, transduced cells were selected with puromycin (1µg/ml) for 10 days. Knock-down efficiency was assessed via both western blot and qRT-PCR analysis (Fig. S1).

RNA isolation and quantitative Real-Time PCR

Total RNA was extracted with TRIzol Reagent (Thermo Fisher Scientific, 15596018) and reverse transcribed using High-Capacity cDNA Reverse Transcription kit (Applied Biosystems, 4368814) according to manufacturer's instructions. Real-time quantitative PCR (qRT-PCR) was performed according to StepOnePlus system's protocol (Applied Biosystems) with SensiFAST SYBR Hi-ROX Kit (Meridian Bioscience, Cincinnati, OH, BIO-92020). C*t* values for each target gene were normalized to *GAPDH* C*t* values. See Supplement Information Table S1 for primers sequence used in this study.

Immunofluorescence

Cells were fixed with 4% formaldehyde (Sigma-Aldrich), permeabilized with 0.1% Triton X-100, then blocked with 1% bovine serum albumin (BSA) in PBS. Cells were stained with primary antibodies Nanog (1:200; rabbit polyclonal, #PA1-097, Thermo Fisher Scientific), Oct4 (1:200; mouse monoclonal, #75463, Cell Signaling), Sox2 (1:500; rabbit monoclonal, #97959, Abcam), TRA1-60 (1:100; mouse monoclonal, #41–100, Life Technologies), Brachyury (1:20; goat polyclonal, #AF2085, R&D System), Sox17 (1:20; goat polyclonal, #AF1924, R&D System), Nestin (1:1000; mouse monoclonal, #60091, Stem Cell Technologies), Nrf2 (1:100; mouse monoclonal, #SC-365949, Santa Cruz) and incubated overnight at 4°C in a blocking buffer. Secondary antibodies goat anti-mouse Alexa-Fluor-488, goat anti-rabbit Alexa Fluor-594 and donkey anti-goat Alexa-Fluor-594 (all from Life Technologies) were used for detection. DAPI (Carl Roth) was used for nuclei counterstain. Images were acquired with a Leica DMi8 inverted microscope. Filter cubes and software (LAS X) from Leica.

Western Blotting

Cells were lysed in RIPA lysis Buffer (Sigma-Aldrich) containing Protease inhibitor cocktail (Thermo Fisher Scientific, 78430). Protein concentration was determined by Bradford Assay (Biorad). Equal amounts of protein were resolved by 12% SDS-PAGE and transferred to a nitrocellulose membrane (Biorad, 1704159). Membranes were blocked at room temperature with TBST (0.1% Tween-20 in TBST) containing 5% milk. Immunoblotting was performed with primary antibodies against FTH1 (Santa Cruz, #376594, 1:200), Nanog (Thermo Fisher Scientific, #PA1-097, 1:500), Nrf2 (Santa Cruz, #SC-365949, 1:100), p62/Sqstm1 (Abcam, #ab56416, 1:1000), Gpx4 (Abcam, #ab41787, 1µg/ml), HIF1 (Cell Signaling, #3716s, 1:1000), FTL (Santa Cruz, #74513, 1:100), Caspase 3 (Cell Signaling, #9669, 1:1000), Akt1 (Cell Signaling, #2967, 1:1000), pAkt1 (Cell Signaling, #4058, 1:1000), Erk1/2 (Cell Signaling, #9107, 1:1000), pErk1/2 (Cell Signaling, #4376, 1:1000), Parp1 (Cell signaling, #9543, 1:1000) overnight at 4°C. After several washes with TBST, membranes were incubated with horseradish peroxidase (HRP)-conjugated secondary antibodies (Jackson ImmunoResearch, West Grove, PA) for 1 h at room temperature. Immunoreactive protein bands were probed using an enhanced chemiluminescence detection system (Biorad, 170–5060)

and acquired with UVITEC 165 Imaging Systems. Gapdh (Bioss, BS-1099 R, 1:1000) or Actin (Santa Cruz, SC-1616, 1:500) antibodies were used indifferently as loading control.

Measurement of intracellular ROS and mitochondrial superoxide species

Total intracytoplasmic ROS as well as specific mitochondrial superoxide species were assessed by flow cytometry using the fluorescent probes 2'-7'- Dichlorodihydrofluorescein diacetate (CM-H2DCFDA; Thermo Fisher Scientific) and MitoSOX™ Red Mitochondrial Superoxide Indicator, respectively. For the quantification of mitochondrial superoxide levels, cells were incubated with 2mM MitoSOX™ Red Mitochondrial Superoxide Indicator (Thermo Fisher Scientific) for 30 minutes at 37°C. Intracellular ROS levels were instead assayed by staining the cells with 1,5 mM CM-H2DCFDA (Thermo Fisher Scientific) for 30 minutes at 37°C. Fluorescence intensity was measured by flow cytometry using a FACS BD LSRFortessaTM X-20 cytofluorimeter (BD Biosciences, Bedford, MA). The results were analyzed with FlowJo software (Tree Star, Inc.). Three independent experiments were conducted.

Analysis of mitochondrial membrane potential (ΔΨ)

Mitochondrial membrane potential (ΔΨ) was measured by using 0,1 ΔΨ fluorescent indicator TMRM (tetramethylrhodamine methyl ester) (Thermo Fisher Scientific). Fluorescence intensity was measured after 30 min of incubation at 37°C by flow cytometry using a FACS BD LSRFortessaTM X-20 cytofluorimeter (BD Biosciences). The results were analyzed with FlowJo software (Tree Star, Inc.). Three independent experiments were conducted.

Embryoid Bodies (EBs) formation Assay

ESCs at ~ 80% confluence were dissociated into single cells with StemPro Accutase (Life Technologies). 1.5 x 10^6 cells were resuspended in Brew medium containing 10 μM Y27632 ROCK inhibitor (Selleckchem, S1049), and cultured onto ultra-low attachment plates (TPP, 93060). Cells were maintained in these conditions for 3 days. After 7 days, floating EBs were plated on laminin-coated dishes (Biolamina, LN521-03) and cultured in DMEM-F12 medium (Gibco, 21331-020) containing 20% Knockout Serum Replacement, KSR (Gibco, 10828-028), 1% Glutamax I-CTS (Gibco, A12860-01), 1% MEM-NEAA (Gibco, 1140-035), 0,1 mM 2-mercaptoethanol (Gibco, 21985-023), and 1% Pen/Strep (Gibco, 15140-122), for 28 days.

Alkaline Phosphatase Assay

Cells were fixed with 3,7% formaldehyde (FA) solution (Sigma Aldrich, 252549-100ML) for 15 minutes at room temperature. Alkaline Phosphatase assay was performed using 1-Step NBT/BCIP (Thermo Fisher Scientific, 34042) according to the manufacturer's instructions.

Metabolic and bioenergetic function profile

Total ATP production rates in H9-shFTH1 and shSCR control cells were measured with the Agilent Seahorse Analyzer as previously described by Zhang et al. [Jin Zhang, 2012] using the XFp Real-Time

Rate Assay Kit. Simultaneous quantification of ATP fractions produced by mitochondrial oxidative phosphorylation (OXPHOS) and glycolysis were detected. For bioenergetics quantification, cells were dissociated into single cells with Accutase and seeded at a cell density of 2 x 10^4/well in Brew medium supplemented with 10 mM Y27632 ROCK inhibitor. The day after, the growth medium was exchanged with unbuffered media and incubated for 30 minutes at 37°C allowing temperature and pH to reach the equilibrium before starting the baseline measurements. Once the basal oxygen consumption rate (OCR) and extracellular acidification rate (ECAR) were obtained, cells were metabolically perturbed by the additions of three different compounds: Oligomycin (1.5 µM), Rotenone + Antimycin A (0.5 µM). Finally, the template was loaded into the Seahorse Analyzer for ATP measurement. The same procedure for cell preparation was used for the Glycolytic rate assay and measurement performed according to the manufacturer's instruction. Rotenone/antimycin A were used to block mitochondrial activity while 2-DG to inhibit glycolysis. Results were uploaded to Agilent Seahorse Analytics to calculate parameters relative to ATP production and XF Glycolytic Rate assays. GraphPad Prism software was used to create graphs.

Statistics

All statistical data were generated from at least three independent biological replicates and are represented as mean ± standard error of the mean (SEM). Data were analyzed with PRISM version 7.0 (GraphPad Software Inc., San Diego, CA, USA). The significance of differences (*p*-value) was analyzed using Student's *t*-test and presented with the following levels of significance: **P* < 0.05, ***P* < 0.01, and ****P* < 0.001.

Results

FTH1-silencing mediates impairment of ESCs pluripotency.

Iron homeostasis is involved in many biological processes including the maintenance of pluripotency in human PSCs. For instance, results from previous research found that depletion of intracellular iron associates with impairment of pluripotency and self-renewal due to significant reduction of *NANOG* expression (25). Cells maintain a balanced iron pool and in this regulation ferritin, as iron storage protein, plays a crucial role. Therefore, to speculate on the role of ferritin in the context of hESCs, we first generated FTH1-silenced cells via lentiviral transfection with short hairpin RNA (shRNA); subsequent analysis at both mRNA and protein levels confirmed that *FTH1* was successfully knocked-down in transfected hESC (Supplementary Fig. S1B-S1E). Morphologically, colonies from FTH1-KD hESCs were more flattened than those of shSCR control (Supplementary Fig. S1A), and alkaline phosphatase (AP) activity was reduced in FTH1-silenced cells (Fig. 1A). FTH1-KD hESCs colonies were positive for pluripotency markers Oct4, TRA-1-60, and Sox2, while the expression of Nanog was slightly increased (Fig. 1B and Supplementary Fig. S2A). This last finding was further confirmed by immunoblot analysis demonstrating that Nanog expression is indeed higher in FTH1-silenced hESCs. (Fig. 1C). At the transcriptional level, *OCT4*, *SOX2*, and *NANOG* resulted evenly increased in FTH1-KD hESCs (Fig. 1D). We further asked whether *FTH1* knockdown could, either directly or indirectly, promote spontaneous

differentiation of hESCs. Analysis of the transcript levels of *AFP*, *Nkx2*.5, and *PAX6*, specific of endoderm, mesoderm, and ectoderm germ layers respectively, revealed an enhanced expression of these genes in FTH1-KD hESCs (Fig. 1E, left panel). Next, we induced both SCR control and FTH1-KD hESCs to differentiate using the Embryoid bodies (EBs) formation method (Supplementary S2B). On day 28 of differentiation, EBs were harvested and analyzed for endodermal- (*GATA4, FOXA2*), mesodermal- (*HAND1*, *CD31*), and ectodermal- (*NESTIN, PAX6*) associated markers. While endodermal and mesodermal transcript levels resulted upregulated in FTH1-KD-derived EBS compared to control EBs, the ectodermal genes *NESTIN* and *PAX6* were significantly downregulated in EBs derived from silenced cells (Fig. 1E, right panel), suggesting that modulation of *FTH1* by repression negatively affects neuroectodermal gene expression. Immunofluorescence analysis for Sox17 (endodermal marker), Brachyury (mesodermal marker), and Nestin further confirmed that the percentage of $Nestin^{+}$ cells is lower in FTH1-silenced hESCs compared to SCR control (Fig. 1F). A similar pattern of results was observed in a previous study, in which overexpression of *NANOG* was associated with neuroectodermal differentiation impairment of hESCs (80).

ROS levels are reduced upon FTH1-gene silencing in hESCs

The role of ferritin in preventing iron-mediated oxidative stress was observed in many studies reporting a direct correlation between modulation of *FTH1* expression and dysregulation of iron homeostasis (75). Specifically, a reduction in *FTH1* expression leads to excess labile iron, in turn promoting the formation of oxygen-derived free radicals (39, 67). To speculate on the effects of *FTH1* silencing in hESCs, we measured total and mitochondrial ROS levels together with an analysis of the mitochondrial membrane potential (ΔΨM) on three biological replicates of SCR and FTH1-KD hESCs, using DCF, MitoSox, and TMRM dyes, respectively (Supplementary S3A and S3B). Intriguingly, our data revealed a reduction in total ROS levels in FTH1-silenced hESCs compared to SCR controls (FTH1-KD: CM-H2DCFDA MFI: 29785,7 *vs* SCR: CM-H2DCFDA MFI: 47341,7) (Fig. 2A). Likewise, MitoSox assay highlighted a significant reduction in mitochondrial superoxide in FTH1-deficient cells (FTH1-KD: MitoSOX Red MFI: 251,8 *vs* SCR: MitoSOX Red MFI: 1002,3) (Fig. 2B). A similar, asymmetric behavior was observed by flow cytometry analysis, which revealed a decrease in TMRM fluorescence, indicative of mitochondrial membrane depolarization, in FTH1-KD hESCs (MFI: 7722) compared to SCR control (MFI: 11086,7) (Fig. 2C). Together, these results led us to conclude that hESCs had to operate and overactivate well established antioxidant systems in order to protect themselves from shFTH1-mediated iron toxicity.

Nrf2 signaling pathway drives the antioxidant response in hESCs

The nuclear factor (erythroid 2-related) factor 2 (Nrf2) is a transcription factor ubiquitously expressed in most eukaryotic cells. Nrf2-Keap1 (Kelch-like ECH-associated protein 1) signaling pathway was shown to play a central role in protecting cells against oxidative stress (41, 50). Under basal conditions, Nrf2 is bound to its negative regulator Keap1 which directs it to proteasomal degradation. In the presence of

intracellular ROS, Keap1 is oxidized and releases Nrf2 which is free to translocate into the nucleus, where it binds to antioxidant response elements (AREs) and induces the expression of antioxidant target genes, such as *HMOX1, NQO1, GST, GPX* (36). Besides its role as a fine regulator of redox and metabolic homeostasis, Nrf2 also acts as a pluripotency master gene: Nrf2 activation in hESCs was shown to enhance *NANOG* transcriptional activity by delaying Nanog protein degradation through POMP-mediated proteasome ubiquitination (27, 33). We found that FTH1-KD hESCs express higher levels of Nrf2 transcript (Fig. 3A) and protein (Fig. 3B and 3C; Supplementary Fig. S4A), assessed via qRT-PCR, immunoblot, and immunofluorescence (Supplementary Fig. S4F), respectively. Similarly, we could also observe an increased expression of p62/Sqstm1 (Fig. 3D and Supplementary Fig. S4B) which, in the non-canonical Keap1-Nrf2 pathway, is known to bind Keap1, allowing Nrf2 to migrate into the nucleus (37). Moreover, the p62 protein yields a feedback loop that amplifies the Nrf2 system (32). In addition to increased expression of Nrf2 in FTH1-silenced hESCs, we observed the overexpression of some important antioxidant enzymes, such as glutathione peroxidases Gpx2, Gpx3 (Fig. 3E), Gpx4 (Fig. 3F and Supplementary Fig. S4C), and superoxide dismutases (Sod) 1 and 2 (Fig. 3G). Also, more Nrf2-regulated genes (*HMOX1*, *NQO1*, *HIF1α*, *HIF2α*) (Fig. 3H) and proteins (Hif1α, Ftl) (Fig. 3I and Fig. 3L, respectively and Supplementary Fig. S4D and S4E) were found highly expressed in FTH1-KD hESCs. Altogether, these findings suggest a crosstalk between *FTH1* silencing and overactivation of the Nrf2 signaling pathway and its cognate effectors in hESCs.

FTH1 knock-down triggers Apoptosis and DNA damage

Labile iron accumulation is a well-known cell damage effector and pro-apoptotic factor (13, 35, 74); intracellular iron overload by ferric ammonium citrate (FAC) treatment leads to ferroptosis, an iron-regulated cell death (15). To check the effects of FTH1-silencing on apoptosis, expression analysis of intrinsic pro-apoptotic genes such as *BAX* and *BIM*, as well as *CASP9* and *CASP3* was performed, revealing a significant upregulation of their expression in FTH1-KD with respect to SCR control hESCs (Fig. 4A and 4B). Similarly, immunoblot analysis of cleaved Casp3 protein confirmed its overexpression in silenced hESCs (Fig. 4C and Supplementary Fig. S5A). It is by now generally accepted that Akt and Erk1/2 pathways are both linked to apoptosis, but with opposite effects: Erk promotes apoptosis, both intrinsically and extrinsically and its activity can be driven by the presence of ROS (90). By contrast, Akt is linked to cell survival, therefore its activity mediates suppression of apoptosis (38). Based on these observations, we speculated whether Erk and Akt could be involved in our FTH1-KD hESCs system; therefore, we measured their expression levels by immunoblot analysis and found that the active, phosphorylated Akt protein (pAkt) expression was reduced, while the expression of pErk1/2 resulted significantly increased in FTH1-silenced hESCs (Fig. 4D and 4E, respectively; Supplementary Fig. S5B and S5C). Collectively, these findings clearly suggest that an active cell death program occurs in hESCs when ferritin is stably downregulated. In addition, based on the evidence that high ROS levels and *FTH1* modulation also associate with DNA damage (8, 65, 73, 83), we measured the expression of some DNA damage-associated genes. In line with previous studies, here we show that *BRCA1*, *DMC1*, *PCNA*, and *POLQ* are indeed significantly upregulated in FTH1-KD hESCs (Fig. 4F). Similarly, we could also observe

an increased expression of Parp1 protein, a substrate of activated caspase 3, in FTH1-silenced hESCs (Fig. 4G and Supplementary Fig. S5D). Overall, these results provide strong evidence that *FTH1* silencing induces apoptosis in hESCs and triggers the activation of DNA-damage response programs.

Effects of FTH1 repression on cellular metabolism

Under oxidative stress conditions, a metabolic shift from OXPHOS to glycolysis was reported to occur (87), suggesting a clear and intimate correlation between oxidative stress and metabolic changes. It is also well known that hPSCs rely on glycolysis while OXPHOS takes place as soon as these cells enter differentiation (77, 79). By using the Agilent Seahorse analyzer, we first quantified the fraction of ATP generated by glycolysis and by OXPHOS. The difference between SCR control and FTH1-silenced hESCs in glycolysis *vs*. OXPHOS ATP fraction was negligible. However, we noticed an overall reduction of total ATP production from both sources (Fig. 5A and Supplementary Fig. S6A). We further sought to speculate on the total glycolytic activity in the two groups of cells (shFTH1 *vs*. SCR). A lower basal and compensatory glycolytic rate was detected in FTH1-silenced hESCs, suggesting that mitochondrial respiration is somehow inhibited in these cells which retain the capability to manage energy demand despite the genetic modification in the ferritin gene (Fig. 5B and Supplementary Fig. S6B). For a more comprehensive metabolic investigation, we analyzed the expression levels of glycolysis-specific genes such as *ALDOA, PGK1, ENO1, PKM*, together with genes encoding for enzymes of gluconeogenesis, *G6PC1* and *FBP1*. In line with the results obtained by the glycolytic rate analysis, we could not observe significant changes in the expression of glycolytic genes between SCR and FTH1-silenced hESCs (Fig. 5C); on the other hand, the expression of *G6PC1* (Glucose-6-Phosphatase Catalytic Subunit 1) resulted significantly higher in FTH1-silenced cells (Fig. 5D). *G6PC1* encodes one of the key enzymes responsible for glucose production from glucose-6-phosphate, and therefore is critically involved in glucose homeostasis. This finding perfectly matches with the fact that high glucose levels are required for the proper functionality of detox systems, such as pentose phosphate pathway (PPP), glucuronidation pathway, and glutathione biosynthesis pathway, all of which are regulated by the Nrf2 signaling pathway (29, 51). In support of this, we found that *G6PD* (glucose-6-phosphate dehydrogenase) and *PGD* (6-Phosphogluconate dehydrogenase), two key enzymes involved in PPP, were significantly increased in FTH1-silenced cells (Fig. 5E), strengthening the concept that the PPP may represent a crucial metabolic target by which the Nrf2 signaling potentiates the antioxidant response in hPSCs. The expression of *PDK1* (pyruvate dehydrogenase kinase 1) was significantly enhanced in shFTH1-hESCs as well (Fig. 5F); its expression is positively regulated by *HIF1α*, previously shown to participate in ROS-induced metabolic reprogramming, where *PDK1* prevents the pyruvate from entering the TCA cycle (tricarboxylic acid cycle or Krebs cycle) (40). We finally tested the expression level of *UCP2* (Uncoupling protein-2), a protein of the inner mitochondrial membrane, involved in uncoupling OXPHOS from ATP synthesis. Similarly, to *PDK1*, *UCP2* expression was higher in FTH1-silenced hESCs (Fig. 5G). As *PDK1, UCP2* blocks pyruvate entry into the Krebs cycle and shunts it towards the PPP (31, 60, 85). Altogether, our findings are indicative of a metabolic reorganization occurring in response to iron-mediated oxidative stress.

Discussion

Pluripotent stem cells (PSCs), including ESCs and iPSCs, possess the unique and extraordinary self-renewal capability, while maintaining their pluripotency (58). In addition to these properties, PSCs also have the ability to give rise to almost any cell type, both in vivo and in vitro. On the bases of these key features, the PSCs technology holds enormous potential to attempt many research and biomedical applications, including drug screening, development, and repurposing (5, 16, 78, 89), disease modelling (47, 54–56, 70), cell therapy (82), aging (59), and regenerative medicine (57). Although significant progress has been made, many hurdles still need to be overcome to push PSCs technology towards the road to clinical practice. Apart from immunogenicity and genomic instability, undoubtedly representing the two major challenges, the successful differentiation and functional maturation of PSC derivatives must faithfully recapitulate all aspects of somatic cells and tissues, including the metabolic function. For instance, little is known about the role of ferritin heavy chain (*FTH1*), the major ferroxidase protein, in human ESCs homeostasis. Ferritin is composed of 24 heavy and light chains, whose core is able to sequester up to 4500 iron atoms (26). Ferritin heavy chain, in particular, is responsible for the oxidation of ferrous iron [Fe (II)] to less reactive ferric iron [Fe (III)] (81). Even though there is a wide literature suggesting that FTH1 is a major player in protecting cells against oxidative stress (9), so far, its role in embryonic stem cells has not been fully elucidated. As shortly stated above, ROS play a role as second messengers in embryo development (12, 23), and their effects, beneficial or deleterious, depend on the embryo developmental stage. ESCs, compared to most terminally differentiated cells, are extremely resistant to hypoxic stress as they live and greatly proliferate at low oxygen concentration (14, 64), suggesting that ESCs are equipped with a highly efficient antioxidant system (3, 22). Because of its strong ferroxidase activity, *FTH1* is supposed to be one of the major players in this system, maintaining iron in a safe and bioavailable form. To gain insights on the effects of FTH1-mediated control of ROS-induced cellular stress, here we stably silenced the FTH1 gene in H9 hES cell line using the shRNA strategy. Intracellular ROS production, measured in shFTH1-hESC by flow cytometry together with mitochondrial superoxide species, revealed that silenced cells have decreased levels of ROS accumulation. Similarly, mitochondrial membrane potential detected by TMRM assay, revealed that FTH1 silencing produces a decrease in mitochondrial membrane depolarization in shFTH1-hESCs compared to SCR control. By monitoring self-renewal and pluripotency, key findings emerged: morphologically, shFTH1 hESCs were more flattened and had less AP + cells compared to SCR control cells; the core pluripotency genes *OCT4, NANOG*, and *SOX*2 resulted significantly overexpressed in FTH1-silenced cells; Immunoblot analysis of Nanog protein, also revealed an increased expression in silenced cells. As pointed out elsewhere in the text, *NANOG* expression is under the control of the nuclear factor erythroid 2-related factor 2 (Nrf2), a stress-activated transcription factor involved in the cellular response to multiple injuries, among which oxidation is the most prominent. In a recent review, Dai and Coll. (10) summarize Nrf2-Keap1 signaling in the context of stem cell state and function, suggesting that it can serve as a master regulator of stem cell redox and metabolic homeostasis. Nrf2, in fact, can efficiently modulate ESCs and iPSCs pluripotency status by finely tuning *NANOG* and *OCT4* expression through direct binding to upstream regions of these genes and delaying their proteasome-mediated ubiquitination. Our data

showed clear evidence of the increased Nrf2 expression in hESCs, both at mRNA and protein level, upon FTH1 silencing. Overexpression of Nrf2 is therefore responsible for the upregulation of *NANOG*, as well as for the activation of the Gpx4 (glutathione peroxidase 4), ROS scavenger protein. A correlation between activation of Nrf2 and induced expression of *FTH1* was previously reported in mouse embryonic fibroblasts (MEFs) (61). Ferritin is also known to function as an anti-apoptotic protein (4). Accordingly, our results show that FTH1-silencing triggers the activation of apoptosis-associated genes like *BAX*, *BIM*, *CASP3* and *CASP9;* we further deepened our analysis by examination of the AKT and ERK1/2 pathways, which undergo significant perturbations during apoptosis. Previous studies have reported conflicting results, showing that MAPK/ERK and PI3/AKT signaling pathways can be either activated (6) or decreased (2) in mESCs and hESCs upon ROS exposure. Our data indicate that *FTH1* silencing produces a significant reduction of the pAkt, while activating ERK1/2 signaling. Concerning the metabolic point of view, most of the studies have focused on glycolytic metabolism and on its role in maintaining pluripotency as well as the importance of a metabolic shift of somatic cells to enter pluripotency during reprogramming; however, our study went beyond previous reports, speculating whether modulation of *FTH1* by repression impacts hESCs homeostasis and metabolic properties. Interestingly, extensive analyses carried out showed that FTH1-silenced hESCs undergo metabolic reorganization. We observed that sh-treated hESCs cells respond to *FTH1* silencing by activation of antioxidant systems including enzymes such as *SODs*, *CAT*, and *GPXs*. Moreover, FTH1-silenced hESCs had an increased expression of *G6PD* gene which is one of the major sources of NADPH, essential for maintaining the redox homeostasis (72). Together with *G6PD, PDK1* and *UCP2* were upregulated as well in silenced cells, suggesting a rerouting of metabolites from glycolysis to PPP and corroborated by a reduced glycolytic flux in shFTH1-hESCs. Consistent with the idea that PPP flux leads to an elevated reduction of NADP + to NADPH (21, 63), we suggest that an increased PPP flux is favored in hESCs with repressed FTH1 expression to drive the ROS clearance.

Conclusion

To our knowledge, this is the first study uncovering the role of ferritin modulation by repression in human ESCs. In agreement with our work, previous studies have reported that ESCs are very resistant to oxidative stress. Interestingly, here we provide evidence of a potential interplay between the Nrf2 axis and oxidative pentose phosphate pathway (PPP) as molecular mechanism underlying the antioxidant response in hESCs in a shFTH1-induced stress condition (Fig. 6). Future investigations are necessary to validate the conclusion that can be drawn from this study.

Abbreviations

hESCs: Human embryonic stem cells; FTH1: Ferritin Heavy Chain; ROS: Reactive oxygen species; shRNA: Short Hairpin RNA; KD: Knockdown; SCR: Scramble; NRF2: Nuclear factor erythroid-derived 2-like 2; NF-kB: Nuclear factor kappa B; SOD1: Superoxide Dismutase 1; GPX: Glutathione peroxidase; CAT: Catalase; DFO: Deferoxamine; iPSCs: Induced pluripotent stem cells; PSCs: Pluripotent stem cells; OXPHOS:

Oxidative phosphorylation; ATP: Adenosine triphosphate; HIF1A: Hypoxia inducible factor 1 subunit alpha; NADPH: Nicotinamide adenine dinucleotide phosphate; MFA: Metabolic flux analysis; AP: Alkaline phosphatase; EBs: Embryoid bodies; DCF-DA: 2'-7'-dichlorofluoresceindiacetate; MitoSox: Mitochondrial superoxide; TMRM: Tetramethylrhodamine methyl ester; Keap1: Kelch-like ECH-associated protein 1; HMOX1: Heme oxygenase 1; GST: Glutathione S-transferase; qRT-PCR: Quantitative reverse transcription-polymerase chain reaction; p62/SQSTM1: Sequestome 1; pAKT: phospho-AKT; pERK: phospho-ERK; FACS: Fluorescence-activated cell sorting; ΔΨM: mitochondrial membrane potential; Fe (II): Ferrous ion; Fe (III): Ferric ion; BSA: bovine serum album; TBST: Tris-buffered saline buffer containing 0.1% Tween-20; PPP: pentose phosphate pathway.

Declarations

Ethics approval and consent to participate

The 'Magna Graecia' University of Catanzaro and the Azienda Ospedaliero—Universitaria 'Mater Domini' approved the study and confirmed that all experiments and methods on human embryonic stem cells were carried out according to the World Medical Association Declaration of Helsinki.

This manuscript does not report on the use of animal data.

Consent for Publication

Not relevant

Competing interests

The authors confirm that there are no conflicts of interest.

Acknowledgments

Not applicable.

Data Availability

The processed and normalized data supporting the conclusions of this article are included within the article (Supplementary files). Raw data used during the current study are available from the corresponding author upon reasonable request.

Funding

This study was supported in part by grant # PRIN 2017CH4RNP_001 to G.C.

Authors' contributions

GC and EIP conceptualized, designed and supervised the study; EIP, LS, and VL conceived the experiments; LS, VL carried out most of the experiments with the support of MLC and CZ; EIP, LS, VL, and SS analyzed the data; FB and AS performed cytofluorimetric analysis and analyzed the relative data; EIP, GC, and VL were involved in drafting the manuscript and reviewed its intellectual content; FSC critically reviewed the manuscript; GC was responsible for funding acquisition. All co-authors have reviewed the manuscript and approved its content prior to submission. All co-authors confirm that the manuscript has been submitted solely to this journal and is not published, in press, or submitted elsewhere.

References

1. Aisen P, Enns C, and Wessling-Resnick M. Chemistry and biology of eukaryotic iron metabolism. *Int J Biochem Cell Biol* 33: 940–959, 2001.
2. Armstrong L, Hughes O, Yung S, Hyslop L, Stewart R, Wappler I, Peters H, Walter T, Stojkovic P, Evans J, Stojkovic M, and Lako M. The role of PI3K/AKT, MAPK/ERK and NFκβ signalling in the maintenance of human embryonic stem cell pluripotency and viability highlighted by transcriptional profiling and functional analysis. *Hum Mol Genet* 15: 1894–1913, 2006.
3. Armstrong L, Tilgner K, Saretzki G, Atkinson SP, Stojkovic M, Moreno R, Przyborski S, and Lako M. Human Induced Pluripotent Stem Cell Lines Show Stress Defense Mechanisms and Mitochondrial Regulation Similar to Those of Human Embryonic Stem Cells. *STEM CELLS* 28: 661–673, 2010.
4. Aung W, Hasegawa S, Furukawa T, and Saga T. Potential role of ferritin heavy chain in oxidative stress and apoptosis in human mesothelial and mesothelioma cells: implications for asbestos-induced oncogenesis. *Carcinogenesis* 28: 2047–2052, 2007.
5. Avior Y, Sagi I, and Benvenisty N. Pluripotent stem cells in disease modelling and drug discovery. *Nat Rev Mol Cell Biol* 17: 170–182, 2016.
6. Burdon T, Smith A, and Savatier P. Signalling, cell cycle and pluripotency in embryonic stem cells. *Trends Cell Biol* 12: 432–438, 2002.
7. Caiazza C, D'Agostino M, Passaro F, Faicchia D, Mallardo M, Paladino S, Pierantoni GM, and Tramontano D. Effects of Long-Term Citrate Treatment in the PC3 Prostate Cancer Cell Line. *Int J Mol Sci* 20: 2613, 2019.
8. Cal M, Matyjaszczyk I, Litwin I, Augustyniak D, Ogórek R, Ko Y, and Ułaszewski S. The Anticancer Drug 3-Bromopyruvate Induces DNA Damage Potentially Through Reactive Oxygen Species in Yeast and in Human Cancer Cells. *Cells* 9: 1161, 2020.
9. Cheng H-T, Yen C-J, Chang C-C, Huang K-T, Chen K-H, Zhang R-Y, Lee P-Y, Miaw S-C, Huang J-W, Chiang C-K, Wu K-D, and Hung K-Y. Ferritin heavy chain mediates the protective effect of heme oxygenase-1 against oxidative stress. *Biochim Biophys Acta BBA - Gen Subj* 1850: 2506–2517, 2015.
10. Dai X, Yan X, Wintergerst KA, Cai L, Keller BB, and Tan Y. Nrf2: Redox and Metabolic Regulator of Stem Cell State and Function. *Trends Mol Med* 26: 185–200, 2020.

11. De Angelis MT, Santamaria G, Parrotta EI, Scalise S, Lo Conte M, Gasparini S, Ferlazzo E, Aguglia U, Ciampi C, Sgura A, and Cuda G. Establishment and characterization of induced pluripotent stem cells (iPSCs) from central nervous system lupus erythematosus. *J Cell Mol Med* 23: 7382–7394, 2019.
12. Dennery PA. Effects of oxidative stress on embryonic development. *Birth Defects Res Part C Embryo Today Rev* 81: 155–162, 2007.
13. Dixon SJ and Stockwell BR. The role of iron and reactive oxygen species in cell death. *Nat Chem Biol* 10: 9–17, 2014.
14. Ezashi T, Das P, and Roberts RM. Low O2 tensions and the prevention of differentiation of hES cells. *Proc Natl Acad Sci* 102: 4783–4788, 2005.
15. Fang S, Yu X, Ding H, Han J, and Feng J. Effects of intracellular iron overload on cell death and identification of potent cell death inhibitors. *Biochem Biophys Res Commun* 503: 297–303, 2018.
16. Fiedler LR, Chapman K, Xie M, Maifoshie E, Jenkins M, Golforoush PA, Bellahcene M, Noseda M, Faust D, Jarvis A, Newton G, Paiva MA, Harada M, Stuckey DJ, Song W, Habib J, Narasimhan P, Aqil R, Sanmugalingam D, Yan R, Pavanello L, Sano M, Wang SC, Sampson RD, Kanayaganam S, Taffet GE, Michael LH, Entman ML, Tan T-H, Harding SE, Low CMR, Tralau-Stewart C, Perrior T, and Schneider MD. MAP4K4 Inhibition Promotes Survival of Human Stem Cell-Derived Cardiomyocytes and Reduces Infarct Size In Vivo. *Cell Stem Cell* 24: 579-591.e12, 2019.
17. Folmes CDL, Dzeja PP, Nelson TJ, and Terzic A. Metabolic Plasticity in Stem Cell Homeostasis and Differentiation. *Cell Stem Cell* 11: 596–606, 2012.
18. Forrester SJ, Kikuchi DS, Hernandes MS, Xu Q, and Griendling KK. Reactive Oxygen Species in Metabolic and Inflammatory Signaling. *Circ Res* 122: 877–902, 2018.
19. Forsyth NR, Musio A, Vezzoni P, Simpson AHRW, Noble BS, and McWhir J. Physiologic Oxygen Enhances Human Embryonic Stem Cell Clonal Recovery and Reduces Chromosomal Abnormalities. *Cloning Stem Cells* 8: 16–23, 2006.
20. Galaris D, Barbouti A, and Pantopoulos K. Iron homeostasis and oxidative stress: An intimate relationship. *Biochim Biophys Acta BBA - Mol Cell Res* 1866: 118535, 2019.
21. Grant CM. Metabolic reconfiguration is a regulated response to oxidative stress. *J Biol* 7: 1, 2008.
22. Guo Y-L, Chakraborty S, Rajan SS, Wang R, and Huang F. Effects of Oxidative Stress on Mouse Embryonic Stem Cell Proliferation, Apoptosis, Senescence, and Self-Renewal. *Stem Cells Dev* 19: 1321–1331, 2010.
23. Han Y, Ishibashi S, Iglesias-Gonzalez J, Chen Y, Love NR, and Amaya E. Ca2+-Induced Mitochondrial ROS Regulate the Early Embryonic Cell Cycle. *Cell Rep* 22: 218–231, 2018.
24. Han Z, Xu Z, Chen L, Ye D, Yu Y, Zhang Y, Cao Y, Djibril B, Guo X, Gao X, Zhang W, Yu M, Liu S, Yan G, Jin M, Huang Q, Wang X, Hua B, Feng C, Yang F, Ma W, and Liu Y. Iron overload inhibits self-renewal of human pluripotent stem cells via DNA damage and generation of reactive oxygen species. *FEBS Open Bio* 10: 726–733, 2020.
25. Han Z, Yu Y, Xu J, Bao Z, Xu Z, Hu J, Yu M, Bamba D, Ma W, Ding F, Zhang L, Jin M, Yan G, Huang Q, Wang X, Hua B, Yang F, Li Y, Lei L, Cao N, Pan Z, and Cai B. Iron Homeostasis Determines Fate of

Human Pluripotent Stem Cells Via Glycerophospholipids-Epigenetic Circuit: Iron Is Critical for hiPSC/ESC Identity. *STEM CELLS* 37: 489–503, 2019.

26. Harrison PM, Banyard SH, Hoare RJ, Russell SM, and Treffry A. The structure and function of ferritin. *Ciba Found Symp*: 19–40, 1976.
27. Hawkins KE, Joy S, Delhove JMKM, Kotiadis VN, Fernandez E, Fitzpatrick LM, Whiteford JR, King PJ, Bolanos JP, Duchen MR, Waddington SN, and McKay TR. NRF2 Orchestrates the Metabolic Shift during Induced Pluripotent Stem Cell Reprogramming. *Cell Rep* 14: 1883–1891, 2016.
28. Heiden MGV, Locasale JW, Swanson KD, Sharfi H, Heffron GJ, Amador-Noguez D, Christofk HR, Wagner G, Rabinowitz JD, Asara JM, and Cantley LC. Evidence for an Alternative Glycolytic Pathway in Rapidly Proliferating Cells. *Science* 329: 1492–1499, 2010.
29. Heiss EH, Schachner D, Zimmermann K, and Dirsch VM. Glucose availability is a decisive factor for Nrf2-mediated gene expression. *Redox Biol* 1: 359–365, 2013.
30. Holmström KM and Finkel T. Cellular mechanisms and physiological consequences of redox-dependent signalling. *Nat Rev Mol Cell Biol* 15: 411–421, 2014.
31. Iurlaro R, León-Annicchiarico CL, and Muñoz-Pinedo C. Chapter Three - Regulation of Cancer Metabolism by Oncogenes and Tumor Suppressors. In: *Methods in Enzymology*, edited by Galluzzi L and Kroemer G. vol. 542Academic Press, 2014, pp. 59–80.
32. Jain A, Lamark T, Sjøttem E, Bowitz Larsen K, Atesoh Awuh J, Øvervatn A, McMahon M, Hayes JD, and Johansen T. p62/SQSTM1 Is a Target Gene for Transcription Factor NRF2 and Creates a Positive Feedback Loop by Inducing Antioxidant Response Element-driven Gene Transcription. *J Biol Chem* 285: 22576–22591, 2010.
33. Jang J, Wang Y, Kim H-S, Lalli MA, and Kosik KS. Nrf2, a Regulator of the Proteasome, Controls Self-Renewal and Pluripotency in Human Embryonic Stem Cells: Nrf2-Proteasome Pathway Controls Stemness in hESCs. *STEM CELLS* 32: 2616–2625, 2014.
34. Ji A-R, Ku S-Y, Cho MS, Kim YY, Kim YJ, Oh SK, Kim SH, Moon SY, and Choi YM. Reactive oxygen species enhance differentiation of human embryonic stem cells into mesendodermal lineage. *Exp Mol Med* 42: 175, 2010.
35. Jin X, He X, Cao X, Xu P, Xing Y, Sui S, Wang L, Meng J, Lu W, Cui R, Ni H, and Zhao M. Iron overload impairs normal hematopoietic stem and progenitor cells through reactive oxygen species and shortens survival in myelodysplastic syndrome mice. *Haematologica* 103: 1627–1634, 2018.
36. Kansanen E, Kuosmanen SM, Leinonen H, and Levonen A-L. The Keap1-Nrf2 pathway: Mechanisms of activation and dysregulation in cancer. *Redox Biol* 1: 45–49, 2013.
37. Katsuragi Y, Ichimura Y, and Komatsu M. Regulation of the Keap1–Nrf2 pathway by p62/SQSTM1. *Curr Opin Toxicol* 1: 54–61, 2016.
38. Kennedy SG, Kandel ES, Cross TK, and Hay N. Akt/Protein Kinase B Inhibits Cell Death by Preventing the Release of Cytochrome *c* from Mitochondria. *Mol Cell Biol* 19: 5800–5810, 1999.
39. Kerins MJ and Ooi A. The Roles of NRF2 in Modulating Cellular Iron Homeostasis. *Antioxid Redox Signal* 29: 1756–1773, 2018.

40. Kim J, Tchernyshyov I, Semenza GL, and Dang CV. HIF-1-mediated expression of pyruvate dehydrogenase kinase: A metabolic switch required for cellular adaptation to hypoxia. *Cell Metab* 3: 177–185, 2006.
41. Kobayashi A, Kang M-I, Okawa H, Ohtsuji M, Zenke Y, Chiba T, Igarashi K, and Yamamoto M. Oxidative Stress Sensor Keap1 Functions as an Adaptor for Cul3-Based E3 Ligase To Regulate Proteasomal Degradation of Nrf2. *Mol Cell Biol* 24: 7130–7139, 2004.
42. Kondoh H, Lleonart ME, Nakashima Y, Yokode M, Tanaka M, Bernard D, Gil J, and Beach D. A High Glycolytic Flux Supports the Proliferative Potential of Murine Embryonic Stem Cells. *Antioxid Redox Signal* 9: 293–299, 2007.
43. Lees JG, Rathjen J, Sheedy JR, Gardner DK, and Harvey AJ. Distinct profiles of human embryonic stem cell metabolism and mitochondria identified by oxygen. *REPRODUCTION* 150: 367–382, 2015.
44. Lin C-Y, Peng C-Y, Huang T-T, Wu M-L, Lai Y-L, Peng DH, Chen P-F, Chen H-F, Yen BL, Wu KK, and Yet S-F. Exacerbation of Oxidative Stress-Induced Cell Death and Differentiation in Induced Pluripotent Stem Cells Lacking Heme Oxygenase-1. *Stem Cells Dev* 21: 1675–1687, 2012.
45. Lisowski P, Kannan P, Mlody B, and Prigione A. Mitochondria and the dynamic control of stem cell homeostasis. *EMBO Rep* 19: e45432, 2018.
46. Liu K, Cao J, Shi X, Wang L, and Zhao T. Cellular metabolism and homeostasis in pluripotency regulation. *Protein Cell* 11: 630–640, 2020.
47. Lucchino V, Scaramuzzino L, Scalise S, Grillone K, Lo Conte M, Esposito C, Aguglia U, Ferlazzo E, Perrotti N, Malatesta P, Parrotta EI, and Cuda G. Generation of human induced pluripotent stem cell lines (UNIMGi003-A and UNIMGi004-A) from two Italian siblings affected by Unverricht-Lundborg disease. *Stem Cell Res* 53: 102329, 2021.
48. Ma J, Cai H, Wu T, Sobhian B, Huo Y, Alcivar A, Mehta M, Cheung KL, Ganesan S, Kong A-NT, Zhang DD, and Xia B. PALB2 Interacts with KEAP1 To Promote NRF2 Nuclear Accumulation and Function. *Mol Cell Biol* 32: 1506–1517, 2012.
49. Martindale JL and Holbrook NJ. Cellular response to oxidative stress: Signaling for suicide and survival*. *J Cell Physiol* 192: 1–15, 2002.
50. McMahon M, Itoh K, Yamamoto M, and Hayes JD. Keap1-dependent Proteasomal Degradation of Transcription Factor Nrf2 Contributes to the Negative Regulation of Antioxidant Response Element-driven Gene Expression. *J Biol Chem* 278: 21592–21600, 2003.
51. Mitsuishi Y, Taguchi K, Kawatani Y, Shibata T, Nukiwa T, Aburatani H, Yamamoto M, and Motohashi H. Nrf2 Redirects Glucose and Glutamine into Anabolic Pathways in Metabolic Reprogramming. *Cancer Cell* 22: 66–79, 2012.
52. Murry CE and Keller G. Differentiation of Embryonic Stem Cells to Clinically Relevant Populations: Lessons from Embryonic Development. *Cell* 132: 661–680, 2008.
53. Ogasawara MA and Zhang H. Redox Regulation and Its Emerging Roles in Stem Cells and Stem-Like Cancer Cells. *Antioxid Redox Signal* 11: 1107–1122, 2009.

54. Orban M, Goedel A, Haas J, Sandrock-Lang K, Gärtner F, Jung CB, Zieger B, Parrotta E, Kurnik K, Sinnecker D, Wanner G, Laugwitz K-L, Massberg S, and Moretti A. Functional comparison of induced pluripotent stem cell- and blood-derived GPIIbIIIa deficient platelets. *PloS One* 10: e0115978, 2015.
55. Parrotta EI, Lucchino V, Scaramuzzino L, Scalise S, and Cuda G. Modeling Cardiac Disease Mechanisms Using Induced Pluripotent Stem Cell-Derived Cardiomyocytes: Progress, Promises and Challenges. *Int J Mol Sci* 21, 2020.
56. Parrotta EI, Procopio A, Scalise S, Esposito C, Nicoletta G, Santamaria G, De Angelis MT, Dorn T, Moretti A, Laugwitz K-L, Montefusco F, Cosentino C, and Cuda G. Deciphering the Role of Wnt and Rho Signaling Pathway in iPSC-Derived ARVC Cardiomyocytes by In Silico Mathematical Modeling. *Int J Mol Sci* 22: 2004, 2021.
57. Parrotta EI, Scalise S, Scaramuzzino L, and Cuda G. Stem Cells: The Game Changers of Human Cardiac Disease Modelling and Regenerative Medicine. *Int J Mol Sci* 20, 2019.
58. Parrotta EI, Scalise S, Taverna D, De Angelis MT, Sarro G, Gaspari M, Santamaria G, and Cuda G. Comprehensive proteogenomic analysis of human embryonic and induced pluripotent stem cells. *J Cell Mol Med* 23: 5440–5453, 2019.
59. Passaro F and Testa G. Implications of Cellular Aging in Cardiac Reprogramming. *Front Cardiovasc Med* 0, 2018.
60. Pecqueur C, Alves-Guerra M-C, Gelly C, Lévi-Meyrueis C, Couplan E, Collins S, Ricquier D, Bouillaud F, and Miroux B. Uncoupling Protein 2, in Vivo Distribution, Induction upon Oxidative Stress, and Evidence for Translational Regulation*. *J Biol Chem* 276: 8705–8712, 2001.
61. Pietsch EC, Chan JY, Torti FM, and Torti SV. Nrf2 Mediates the Induction of Ferritin H in Response to Xenobiotics and Cancer Chemopreventive Dithiolethiones*. *J Biol Chem* 278: 2361–2369, 2003.
62. Prigione A, Fauler B, Lurz R, Lehrach H, and Adjaye J. The Senescence-Related Mitochondrial/Oxidative Stress Pathway is Repressed in Human Induced Pluripotent Stem Cells. *STEM CELLS* 28: 721–733, 2010.
63. Ralser M and Lehrach H. Building a new bridge between metabolism, free radicals and longevity. *Aging* 1: 836–838, 2009.
64. Rodesch F, Simon P, Donner C, and Jauniaux E. Oxygen measurements in endometrial and trophoblastic tissues during early pregnancy. *Obstet Gynecol* 80: 283–285, 1992.
65. Rowe LA, Degtyareva N, and Doetsch PW. DNA damage-induced reactive oxygen species (ROS) stress response in Saccharomyces cerevisiae. *Free Radic Biol Med* 45: 1167–1177, 2008.
66. Saito S, Lin Y-C, Tsai M-H, Lin C-S, Murayama Y, Sato R, and Yokoyama KK. Emerging roles of hypoxia-inducible factors and reactive oxygen species in cancer and pluripotent stem cells. *Kaohsiung J Med Sci* 31: 279–286, 2015.
67. Salatino A, Aversa I, Battaglia AM, Sacco A, Di Vito A, Santamaria G, Chirillo R, Veltri P, Tradigo G, Di Cello A, Venturella R, Biamonte F, and Costanzo F. H-Ferritin Affects Cisplatin-Induced Cytotoxicity in Ovarian Cancer Cells through the Modulation of ROS. *Oxid Med Cell Longev* 2019: e3461251, 2019.

68. Sanzo MD, Aversa I, Santamaria G, Gagliardi M, Panebianco M, Biamonte F, Zolea F, Faniello MC, Cuda G, and Costanzo F. FTH1P3, a Novel H-Ferritin Pseudogene Transcriptionally Active, Is Ubiquitously Expressed and Regulated during Cell Differentiation. *PLOS ONE* 11: e0151359, 2016.
69. Saretzki G, Walter T, Atkinson S, Passos JF, Bareth B, Keith WN, Stewart R, Hoare S, Stojkovic M, Armstrong L, von Zglinicki T, and Lako M. Downregulation of Multiple Stress Defense Mechanisms During Differentiation of Human Embryonic Stem Cells. *Stem Cells* 26: 455–464, 2008.
70. Scalise S, Scaramuzzino L, Lucchino V, Esposito C, Malatesta P, Grillone K, Perrotti N, Cuda G, and Parrotta EI. Generation of iPSC lines from two patients affected by febrile seizure due to inherited missense mutation in SCN1A gene. *Stem Cell Res* 49: 102083, 2020.
71. Solari C, Petrone MV, Vazquez Echegaray C, Cosentino MS, Waisman A, Francia M, Barañao L, Miriuka S, and Guberman A. Superoxide dismutase 1 expression is modulated by the core pluripotency transcription factors Oct4, Sox2 and Nanog in embryonic stem cells. *Mech Dev* 154: 116–121, 2018.
72. Stincone A, Prigione A, Cramer T, Wamelink MMC, Campbell K, Cheung E, Olin-Sandoval V, Grüning N-M, Krüger A, Alam MT, Keller MA, Breitenbach M, Brindle KM, Rabinowitz JD, and Ralser M. The return of metabolism: biochemistry and physiology of the pentose phosphate pathway. *Biol Rev* 90: 927–963, 2015.
73. Storr HL, Kind B, Parfitt DA, Chapple JP, Lorenz M, Koehler K, Huebner A, and Clark AJL. Deficiency of Ferritin Heavy-Chain Nuclear Import in Triple A Syndrome Implies Nuclear Oxidative Damage as the Primary Disease Mechanism. *Mol Endocrinol* 23: 2086–2094, 2009.
74. Stoyanovsky DA and Billiar TR. Cellular non-heme iron modulates apoptosis and caspase 3 activity. In: *Radicals for Life*. Elsevier, 2007, pp. 253–268.
75. Tian Y, Lu J, Hao X, Li H, Zhang G, Liu X, Li X, Zhao C, Kuang W, Chen D, and Zhu M. FTH1 Inhibits Ferroptosis Through Ferritinophagy in the 6-OHDA Model of Parkinson's Disease. *Neurotherapeutics* 17: 1796–1812, 2020.
76. Trachootham D, Lu W, Ogasawara MA, Valle NR-D, and Huang P. Redox Regulation of Cell Survival. *Antioxid Redox Signal* 10: 1343–1374, 2008.
77. Varum S, Rodrigues AS, Moura MB, Momcilovic O, Easley CA, Ramalho-Santos J, Van Houten B, and Schatten G. Energy Metabolism in Human Pluripotent Stem Cells and Their Differentiated Counterparts. *PLoS ONE* 6: e20914, 2011.
78. Wainger BJ, Kiskinis E, Mellin C, Wiskow O, Han SSW, Sandoe J, Perez NP, Williams LA, Lee S, Boulting G, Berry JD, Brown RH, Cudkowicz ME, Bean BP, Eggan K, and Woolf CJ. Intrinsic Membrane Hyperexcitability of Amyotrophic Lateral Sclerosis Patient-Derived Motor Neurons. *Cell Rep* 7: 1–11, 2014.
79. Wanet A, Arnould T, Najimi M, and Renard P. Connecting Mitochondria, Metabolism, and Stem Cell Fate. *Stem Cells Dev* 24: 1957–1971, 2015.
80. Wang Z, Oron E, Nelson B, Razis S, and Ivanova N. Distinct Lineage Specification Roles for NANOG, OCT4, and SOX2 in Human Embryonic Stem Cells. *Cell Stem Cell* 10: 440–454, 2012.

81. Xu B and Chasteen ND. Iron oxidation chemistry in ferritin. Increasing Fe/O2 stoichiometry during core formation. *J Biol Chem* 266: 19965–19970, 1991.
82. Yamanaka S. Pluripotent Stem Cell-Based Cell Therapy-Promise and Challenges. *Cell Stem Cell* 27: 523–531, 2020.
83. Yu T-W and Anderson D. Reactive oxygen species-induced DNA damage and its modification: A chemical investigation. *Mutat Res Mol Mech Mutagen* 379: 201–210, 1997.
84. Zhang H, Badur MG, Divakaruni AS, Parker SJ, Jäger C, Hiller K, Murphy AN, and Metallo CM. Distinct Metabolic States Can Support Self-Renewal and Lipogenesis in Human Pluripotent Stem Cells under Different Culture Conditions. *Cell Rep* 16: 1536–1547, 2016.
85. Zhang J, Khvorostov I, Hong JS, Oktay Y, Vergnes L, Nuebel E, Wahjudi PN, Setoguchi K, Wang G, Do A, Jung H-J, McCaffery JM, Kurland IJ, Reue K, Lee W-NP, Koehler CM, and Teitell MA. UCP2 regulates energy metabolism and differentiation potential of human pluripotent stem cells. *EMBO J* 30: 4860–4873, 2011.
86. Zhang J, Nuebel E, Daley GQ, Koehler CM, and Teitell MA. Metabolic Regulation in Pluripotent Stem Cells during Reprogramming and Self-Renewal. *Cell Stem Cell* 11: 589–595, 2012.
87. Zheng J. Energy metabolism of cancer: Glycolysis versus oxidative phosphorylation (Review). *Oncol Lett* 4: 1151–1157, 2012.
88. Zhong W, Qian K, Xiong J, Ma K, Wang A, and Zou Y. Curcumin alleviates lipopolysaccharide induced sepsis and liver failure by suppression of oxidative stress-related inflammation via PI3K/AKT and NF-κB related signaling. *Biomed Pharmacother* 83: 302–313, 2016.
89. Zhu Z and Huangfu D. Human pluripotent stem cells: an emerging model in developmental biology. *Development* 140: 705–717, 2013.
90. Zhuang S, Yan Y, Daubert RA, Han J, and Schnellmann RG. ERK promotes hydrogen peroxide-induced apoptosis through caspase-3 activation and inhibition of Akt in renal epithelial cells. *Am J Physiol-Ren Physiol* 292: F440–F447, 2007.

Figures

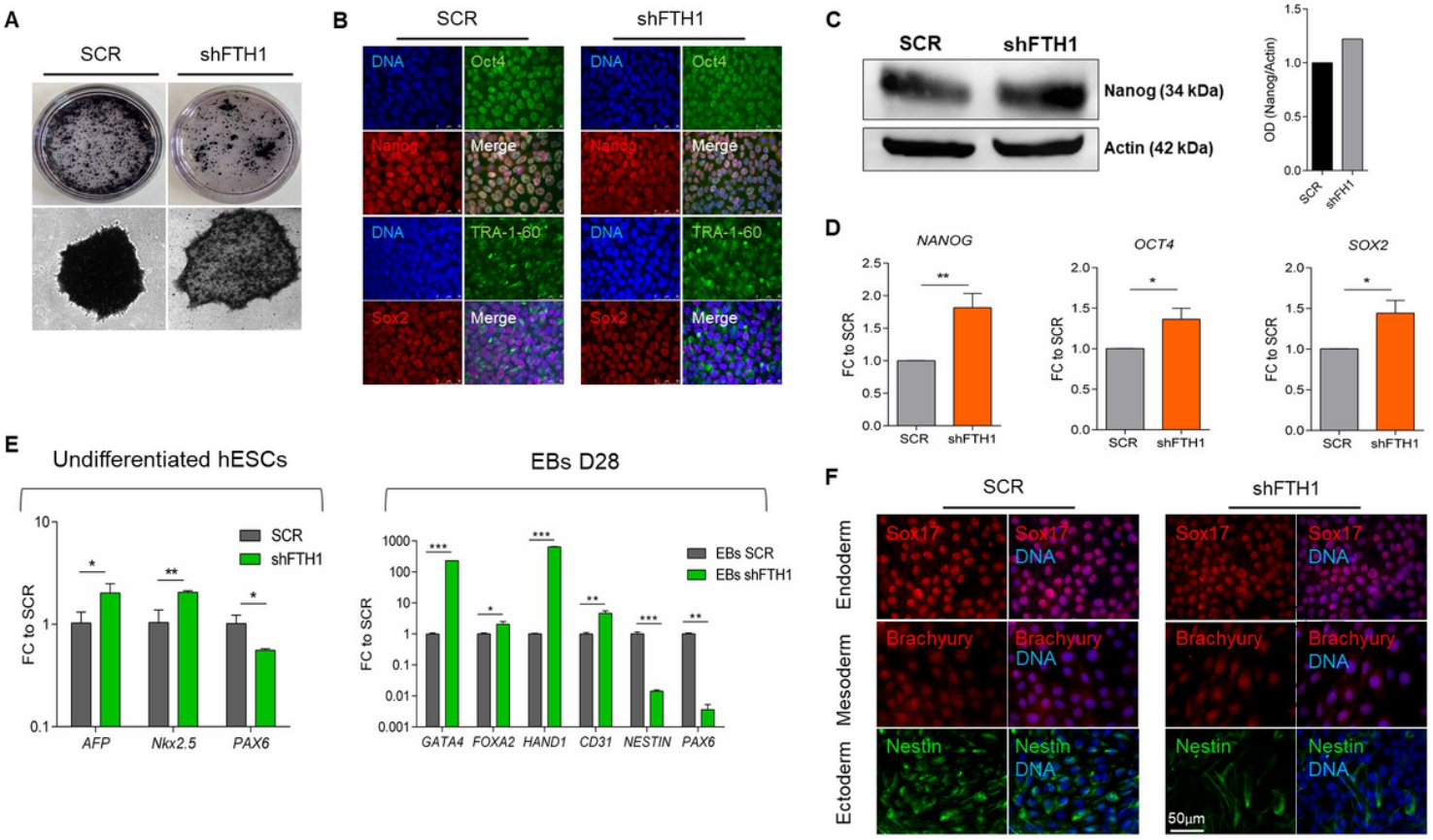

Figure 1

FTH1 silencing influences hESCs pluripotency. (A) Alkaline phosphatase (AP) staining of colonies in SCR control and in hESCs transfected with lentiviral shFTH1 shows that FTH1-silenced ES colonies contain less AP+ cells; scale bars, 250 μm; (B) Undifferentiated SCR and FTH1-KD hESCs were stained for Oct4 (green), Nanog (red), TRA-1-60 (green), and Sox2 (red) expression, while nuclei were counterstained with 4'.6-diamidino-2-phenylindole (DAPI). Scale bars, 50 μm. No significant differences were detected between the two groups with exception for Nanog which shows a slighter positivity in FTH1-silenced cells. C) The levels of Nanog protein were assessed by immunoblotting (IB). Band intensity analysis shows a higher level in FTH1-KD cells compared to SCR control. Actin levels were evaluated to confirm equal loading control. (D) mRNA levels of pluripotency-associated genes NANOG, OCT4, and SOX2 were measured in undifferentiated SCR and FTH1-KD hESCs via qRT-PCR. (E, left panel) mRNA levels of endodermal (AFP), mesodermal (Nkx2.5), and ectodermal (PAX6) genes were measured in undifferentiated SCR and FTH1-silenced hESCs via qRT-PCR analysis; AFP and Nkx2.5 expression levels were higher in shFTH1 cells, while the expression levels of PAX6 was significantly diminished in silenced cells. (E, right panel) mRNA levels of endodermal (GATA4, FOXA2), mesodermal (HAND1, CD31), and ectodermal (NESTIN, PAX6) genes were measured in SCR and FTH1-KD embryoid bodies (EBs) on day 28 of differentiation by qRT-PCR. (F) Sox17, Brachyury, and Nestin, endodermal, mesodermal, and ectodermal markers respectively, were stained via immunofluorescence in SCR and shFTH EBs on day 28 of differentiation; scale bar, 50 μm. Results of all qRT-PCR shown were normalized to value in SCR cells

and are represented as mean ± SEM (n = 3); significance is calculated by t-test: *P ≤ 0.05; **P ≤ 0.01, ***P ≤ 0.001.

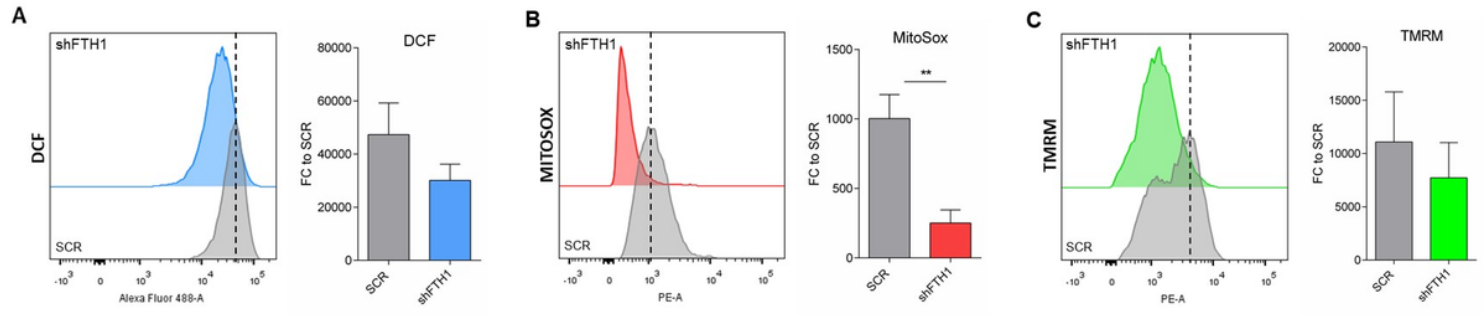

Figure 2

Analysis of ROS levels and mitochondrial functionality in FTH1-KD hESCs. (A) DCF staining showed that total cellular ROS levels are reduced in FTH1-silenced hESCs (light blue curve and bar plot) in respect to control cells. (B) Mitochondrial superoxide resulted significantly lower in FTH1-silenced hESCs (red curve and bar plot), and (C) these cells presented a decrease in mitochondrial membrane depolarization (green curve and bar plot) compared to SCR cells. All data are represented as mean ± SEM (n = 3); **P ≤ 0.01, t-test.

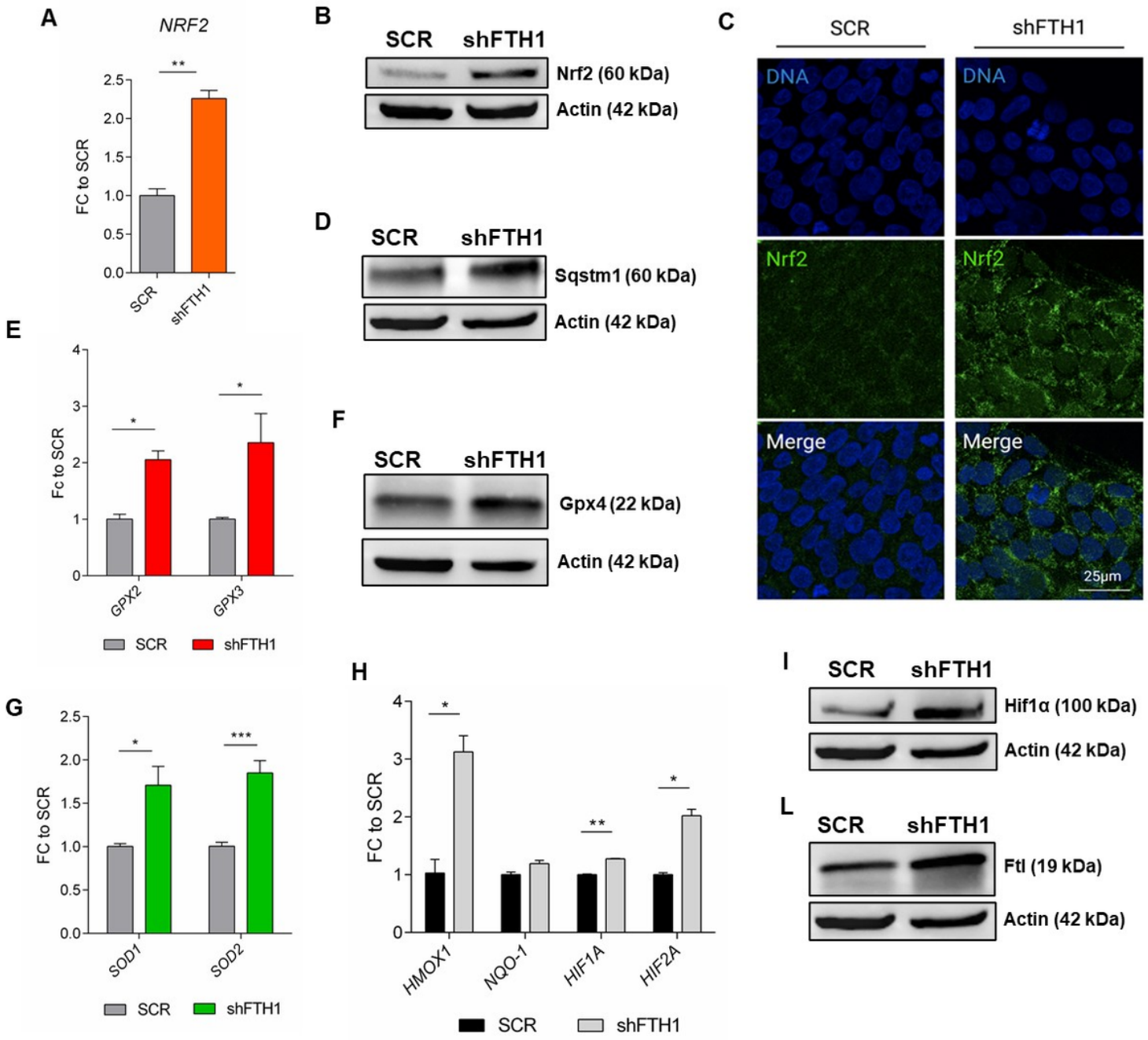

Figure 3

Nrf2 pathway is activated in FTH1-KD hESCs. (A) NRF2 expression was measured in undifferentiated SCR and FTH1-KD hESCs via qRT-PCR, showing a significant up-regulation in presence of FTH1 silencing (B) Nrf2 protein level was assessed by immunoblotting (IB) indicating an increased expression in FTH1-KD hESCs. (C) Immunofluorescence of Nrf2 (green) and nuclei (blue) in SCR control hESCs and FTH1 silenced cells; Scale bars, 25 μm. (D) Immunoblot analysis for p62/Sqstm1 protein in SCR and FTH1-KD cells showing an upregulation of its expression in silenced cells. (E) qRT-PCR analysis of Glutathione peroxidases 2 and 3 (GPX2, GPX3) antioxidant genes in SCR control and FTH1-KD hESCs. (F) Western blot analysis for Gpx4 protein confirming increased expression in FTH1-KD hESCs. (G) qRT-PCR analysis of SOD1 and SOD2 expression in SCR and shFTH1 hESCs showing an upregulation of these genes in

modulated hESCs. (H) mRNA levels of Nrf2 target genes (HMOX1, NQO-1, HIF1A, HIF2A) were measured in SCR and FTH1-KD hESCs via qRT-PCR. (I) Immunoblot analysis of Hif1α and (L) Ftl showed an upregulation of both proteins in FTH1-silenced cells with respect to SCR cells. In all western blots presented in this figure, actin levels were evaluated to confirm equal loading control. For qRT-PCR data were normalized to value in SCR cells and are represented as mean ± SEM (n = 3); significance is calculated by t-test: *P ≤ 0.05; **P ≤ 0.01, ***P ≤ 0.001.

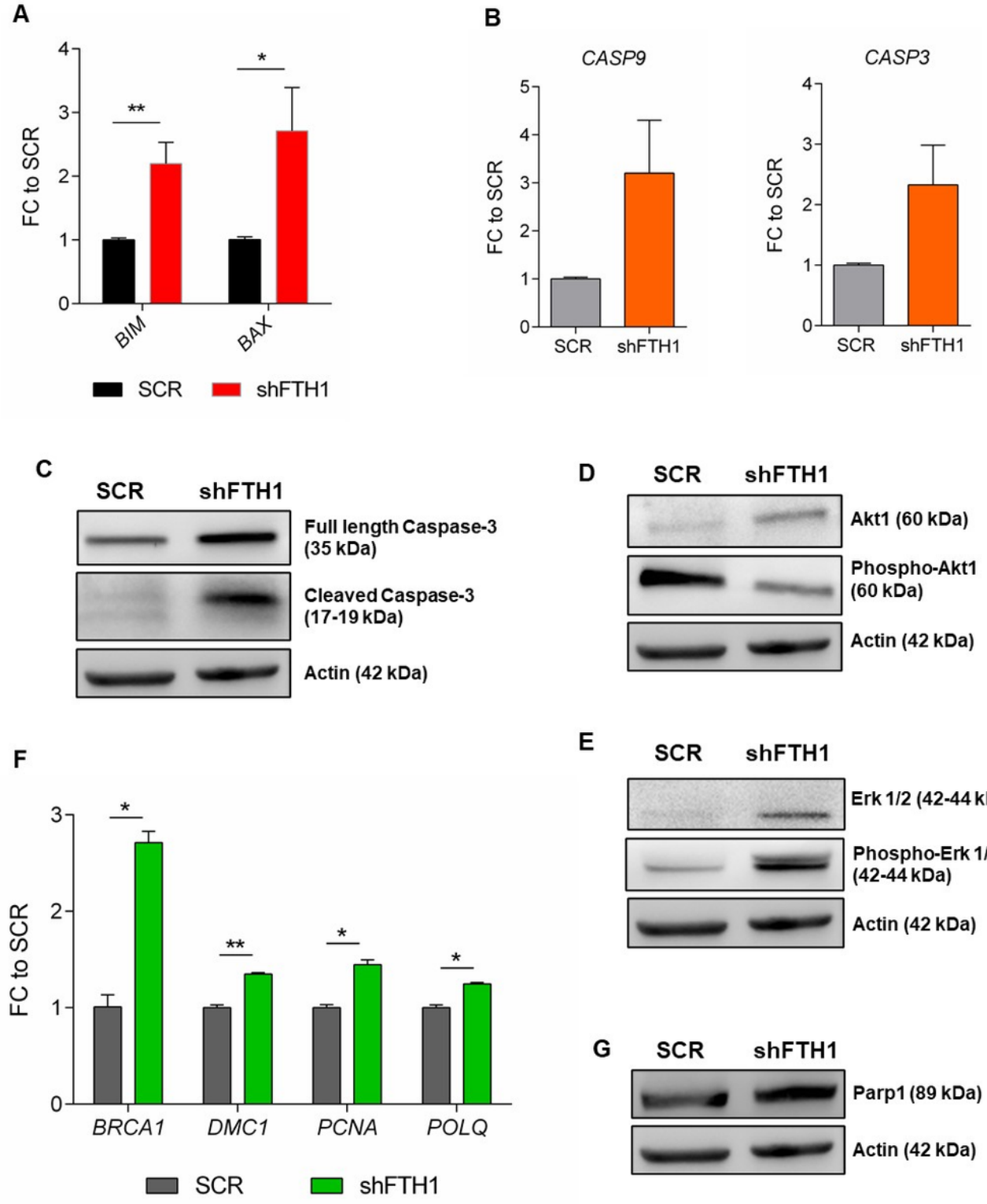

Figure 4

FTH1 silencing leads to expression of apoptosis and DNA damage marker in hESCs. (A) qRT-PCR for apoptosis-associated genes BIM and BAX and (B) CASP3 and CASP9 showing an increased expression levels of apoptotic marker in FTH1-KD hESCs in respect to SCR control. (C) Activation of apoptotic signalling in FTH1-KD hESCs is demonstrated also by immunoblot analysis for full length and cleaved form of Caspase-3. (D) Western blot analysis for Akt1 and phosphorylated Akt1 (Ser473, pAkt) protein expression. (E) immunoblot for total Erk1/2 and phosphorylated Erk1/2 (Thr202/Tyr204, pErk1/2) in SCR control and FTH1-KD hESCs. (F) qRT-PCR analysis for DNA damage related genes (BRCA1, DMC1, PCNA, POLQ) in control and silenced hESCs. (G) Western blot analysis for Parp1 protein expression in SCR and FTH1-silenced cells. For all western blots shown, actin levels were evaluated as loading control. Results of qRT-PCR were normalized to measurements in SCR cells (n = 3); *P ≤ 0.05; **P ≤ 0.01, t-test.

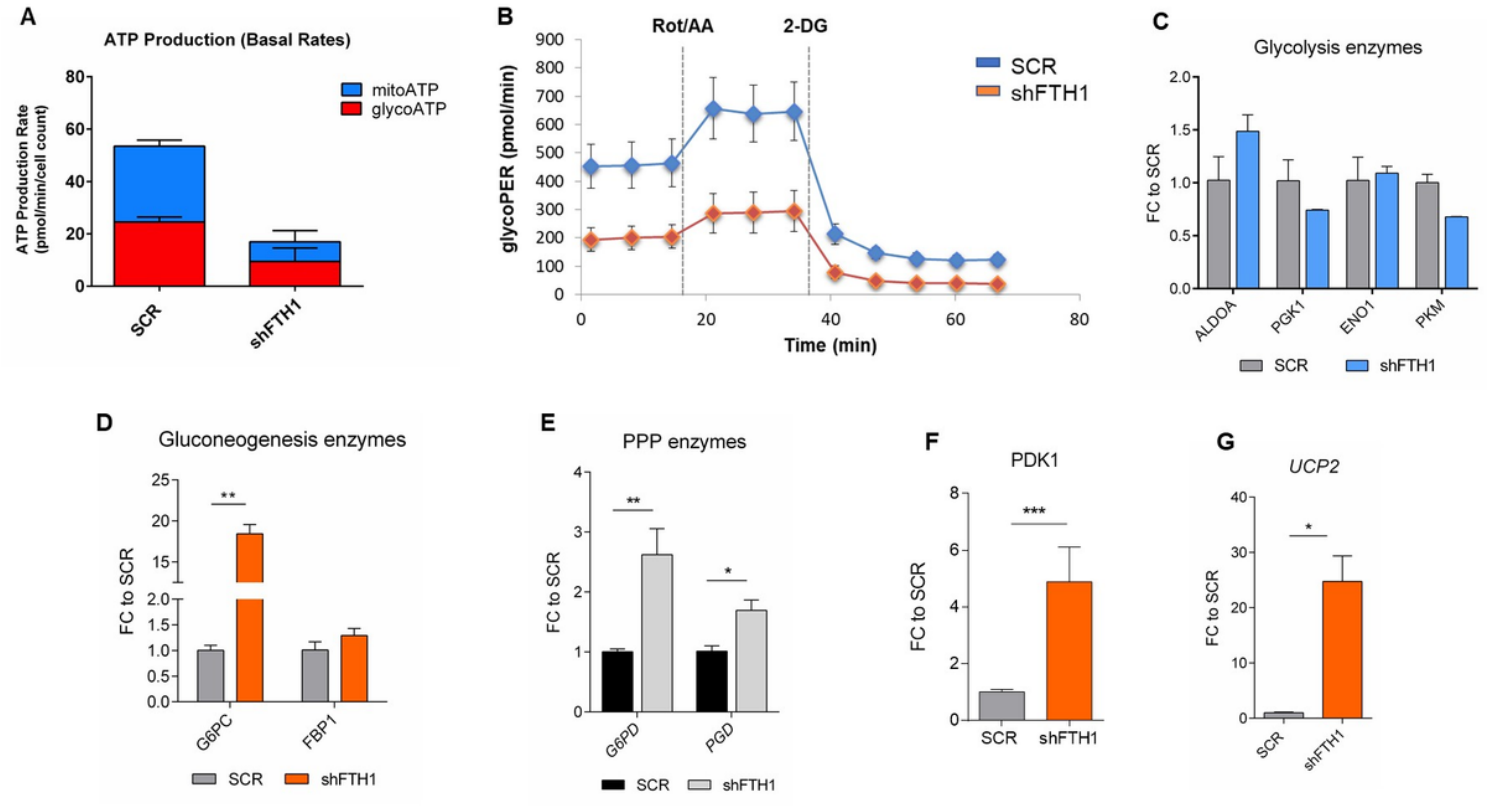

Figure 5

Metabolic rearrangement in FTH1-KD hESCs (A) Quantification of total cellular ATP production (from glycolysis and mitochondrial oxidative phosphorylation) rate using a Seahorse XF analyzer. ATP production was calculated by measuring the oxygen consumption and acidification rate. Each sample (SCR and shFTH1-hESCs) was measured at least in three biological replicates. Seahorse analysis shows a lower ATP production (from both sources) in FTH1-KD cells compared to SCR control. (B) Glycolytic rate measurements in SCR and FTH1-silenced cells calculated by subtracting extracellular acidification rate (ECAR). As shown, FTH1-KD hESCs do not undergo metabolic switch. Since mitochondrial acidification is blocked, the approach measures glycolytic-ECAR only correlating to extracellular lactate accumulation. Glycolytic rate was reduced in FTH1-silenced hESCs. (C) qRT-PCR analysis for glycolytic enzymes (ALDOA2, PGK1, ENO1, and PKM) mRNA expression. (D) Expression of G6PC and FBP1 gluconeogenesis

genes in SCR and shFTH1-hESCs measured by qRT-PCR analysis. (E) Pentose phosphate pathway (PPP) genes G6PD and PGD were significantly up-regulated shFTH1 cells with respect to SCR control cells. (F) The PDK1 gene, responsible for inactivation of pyruvate dehydrogenase and (G) the gene UCP2, that uncouples OXPHOS from ATP synthesis, resulted both significantly up-regulated in FTH1-KD cells compared to SCR cells. For all qRT-PCR graphs, results were normalized to measurements in SCR cells (n = 3); *P ≤ 0.05; **P ≤ 0.01, ***P ≤ 0.001, t-test compared to SCR.

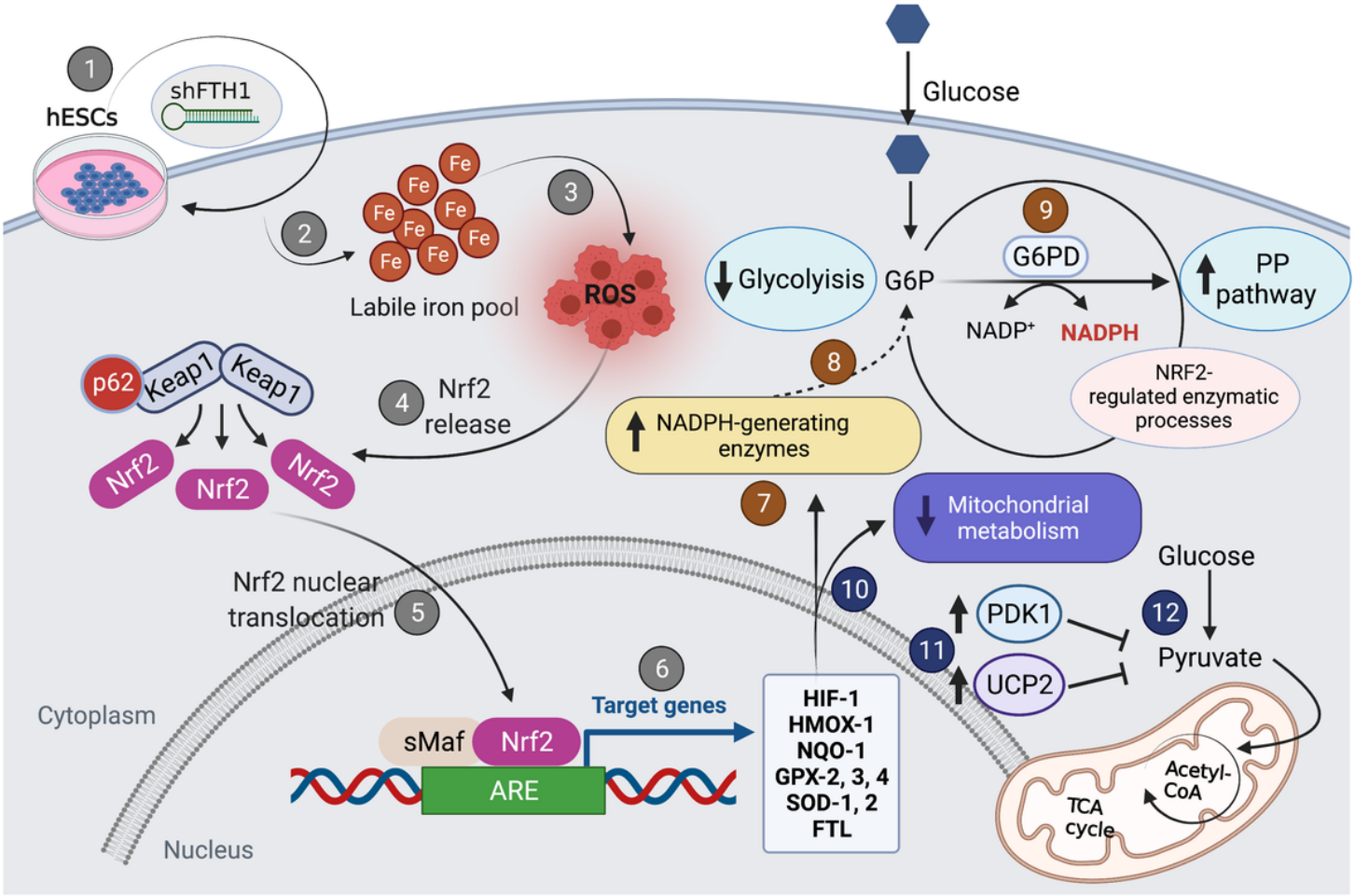

Figure 6

Schematic diagram illustrating oxidative stress response mediated by FTH1 downregulation in hESCs. FTH1 (1) is the master scavenger molecule for intracellular iron homeostasis and its inactivation leads to imbalanced redox homeostasis due to intracellular iron accumulation (2) and ROS production (3). Surprisingly, in hESCs, a reduced expression of FTH1 expression is not associated with oxidative stress and ROS production. This phenomenon can be explained by three crucial findings: first, FTH1-silenced hESCs showed an enhanced transcriptional activity of Nrf2 (4-5) on key antioxidant target genes such as HIF-1, HMOX-1, NQO-1, GPX2/3/4, SOD1/2, FTL (6); second, we observed the activation of an alternative metabolic program from glycolysis (7-8) to pentose phosphate pathway (PPP) where the activity of the G6PD enzyme ensures the conversion of NADP+ to NADPH (9) involved in ROS neutralization; third, the

mitochondrial metabolism was found to be inactive (10) in FTH1-silenced hESCs as demonstrated by the upregulation of PDK1 and UCP2 genes (11), specifically involved in preventing pyruvate to enter into the tricarboxylic acid cycle (TCA) (12).

Supplementary Files

This is a list of supplementary files associated with this preprint. Click to download.

- FigS1.tif
- FigS2.tif
- FigS3.tif
- FigS4.tif
- FigS5.tif
- FigS6.tif
- SupplementaryFigureLegends.docx
- TableS1.docx